Model-based Prognosis Approach using a Zonotopic Kalman Filter with Application to a Wind Turbine

Khoury Boutros[1], Vicenç Puig[1], and Fatiha Nejjari[1]

[1] *Supervision, Safety and Automatic Control Research Center (CS2AC)*
Universitat Politècnica de Catalunya (UPC),
Campus de Terrassa,
Gaia Building, Rambla Sant Nebridi, 22,
08222 Terrassa, Barcelona.
e-mail: boutros.khoury, vicenc.puig, fatiha.nejjari@upc.edu

ABSTRACT

Wind turbines generally operate under adverse conditions making them prone to relatively high failure rates. Due to the direct exposure of the blades to dynamic and cyclic loads of wind, the rotor and the blades unsurprisingly represent the most common major component damages of a wind turbine system, which is especially enhanced when located offshore.

This paper presents a new model-based prognosis procedure based on a zonotopic Kalman filter (ZKF), which combines a physical model with observed data to assess the system degradation. Using this information and the model of the system, the end of life (EOL) and the remaining useful life (RUL) with its uncertainty can be predicted. The proposed prognostic method is applied to monitor the state of health of a wind turbine system specifically, its blades. The remaining useful life prediction will help in scheduling optimal maintenance and reducing the cost caused by wind turbine damage and unplanned shutdown.

1. INTRODUCTION

In recent years, due to the safety and cost benefits involved in adopting a predictive maintenance strategy, research on failure prognosis has been a topic of considerable interest, motivating a plethora of applications to various industrial systems (Ferreira, Balthazar, & Araujo, 2003). Prognostic methods are aimed at predicting the remaining useful life (RUL) of a monitored system, which represents the time before the system reaches a failure state. These methods can be mainly classified into data-driven approaches, model-based approaches or a hybrid of both. Data-driven approaches which is comprehensively reviewed in (Tsui, Chen, Zhou, Hai, & Wang, 2015) use data collected from sensors to extract features which is then used to model the degradation behaviour. On the other hand, model-based approaches use physics-based model of the degradation to assess the RUL of the system. The model-based method has an advantage of incorporating the physical understanding of the monitored system, broadening the scope of investigation, even though the process of development and validation may be tedious and is based on the assumption of a complete knowledge of the physical model (Madhav, 2015). Finally, depending on available output data, a combination of both approaches in a hybrid scheme can be undertaken to achieve an improved predictive performance as done in (Zhang, Kang, & Pecht, 2009).

Prognostic methods should account for the different uncertainties that can influence and affect the predicted RUL which should be as reliable as possible. Uncertainty sources are due to sensor inaccuracy (measurement uncertainty), model uncertainty and future uncertainties due to unknown environment and operating conditions (Gu, Barker, & Pecht, 2007). The main challenge in prognosis is to take these uncertainties into account to obtain a measure of the RUL uncertainty.

In this paper, damage on the blades of wind turbines after repetitive cycle of wind loadings is selected as the health indicator owing to the importance of decreasing cost curves associated with the operation of wind turbines to boast its attractiveness as an alternative source of energy to predominant fossil-based sources, as blades and rotor account for 20% of total cost of wind turbines (IRENA, 2012). By providing important information on RUL, efficient operational planning can be done by operators, decreasing unplanned operational costs.

A model-based prognosis procedure based on the estimation of the EOL and hence the RUL is investigated taking into account damage propagation on the wind turbine blade root. The damage is modelled from stress degradation (Vassilopoulos,

Brøndsted, & Nijssen, 2010) which is a function of the wind speed. Due to the fact that the system states and parameters are essential to this exercise, a zonotopic Kalman filter is designed to estimate the states under the influence of disturbances and noise, with associated bounds accounting for uncertainties which are propagated during prognosis. By evaluating the associated bound, various maintenance decisions can be undertaken, for example, lower bounds can be chosen by operators for conservative purposes. The procedure is then compared with prognosis using the standard Kalman filter for estimation.

2. Model-Based Prognosis

The proposed prognosis approach is primarily based on the model-based architecture as described in (Daigle, Saha, & Goebel, 2012), which has been adapted to the case of a set-based description of uncertainties. When the system in Figure 1 is subject to an input vector $u(k)$, output data $y(k)$ and information from the model, $(x(k), \theta(k)|y_k)$ under uncertainty is used in the estimation of damage aided by the ZKF such that the damage is computed as a bounded set, $\square D(x(k), \theta(k)|y_k)$ from the description of the unknown but bounded uncertainty sets.

This bounded sets' information is subsequently used to calculate the EOL and RUL at a specific time instant k_p that take their values from resultant feasible bounded uncertainty sets, considering their centers as a reference point of estimation, $\square EOL(x(k_p), \theta(k_p)|y(k_p))$ and $\square RUL(x(k_p), \theta(k_p)|y(k_p))$, respectively.

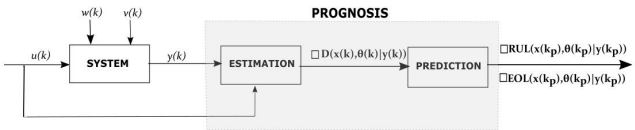

Figure 1. Model-based prognostics architecture.

Given the generic discrete-time model description at time instant k

$$x(k) = f(x(k), \theta(k), u(k), w(k), k), \tag{1a}$$
$$y(k) = h(x(k), \theta(k), u(k), v(k), k). \tag{1b}$$

where $x(k) \in \mathbb{R}^{n_x}$, $\theta(k) \in \mathbb{R}^{n_\theta}$, $u(k) \in \mathbb{R}^{n_u}$ and $w(k) \in \mathbb{R}^{n_x}$ are the states, time varying unknown parameters, inputs and disturbance, respectively, with $y(k) \in \mathbb{R}^{n_y}$ and $v(k) \in \mathbb{R}^{n_y}$ as output and measurement noise at each time instant k. The operation of a model-based prognosis involves predicting forward in time the EOL, based on a physics-based criterion, considering $T_{EOL} \in \mathbb{R}^{n_x} \times \mathbb{R}^{n_\theta}$ as a threshold of failure of a unit under test (UUT), with the main objective of indicating failure over a time history of the UUT when performance of the monitored system is outside the region of the failure threshold T_{EOL}. With the evolution of the performance of the system, $(x(k), \theta(k))$ under the influence of known inputs $u(k)$ and unknown variables, $w(k)$ and $v(k)$, the $T_{EOL} : \mathbb{R}^{n_x} \times \mathbb{R}^{n_\theta} \to \mathbb{B}$ maps to a Boolean domain $\forall \mathbb{B} \coloneqq [0, 1]$, such that a violation of the failure threshold results in $T_{EOL} = 1$ and 0 otherwise. The time of this event of failure of the UUT, at a particular time instant k_p, when system dynamics evolution (1a) in time triggers $T_{EOL} = 1$ is known as the end of life of UUT which is formalised in (Daigle et al., 2012) as

$$EOL(t_p) \coloneqq \inf\{k \in \mathbb{N} : k \geq k_p \wedge T_{EOL}(x(k), \theta(k), u(k)) = 1\},$$

The time before the event of failure, i.e. when $T_{EOL} = 1$, in the present state of the UUT at k_p in future time, is thus given as:

$$RUL(k_p) \coloneqq EOL(k_p) - k_p.$$

3. Zonotopic Kalman Estimation

Considering the fact that the process of estimation of states is crucial in various procedures such as prognosis of systems, the effect of uncertainties on observed states are essential to examine. This warrants state estimation methods, such as the well-established Kalman filter which has seen an abundance of applications over the decades with variant modifications, to enhance its efficiency and alternative uses.

3.1. Background

Different methods of representing these uncertainties motivates different types of estimation schemes. These are mainly through the stochastic paradigm and set-based formulations with the latter involving unknown disturbances and noise that are considered bounded in compact sets. Various geometrical representation for bounded uncertainty sets have been used in a number of works yielding good results. The resultant estimate of set-membership methods are feasible sets that are consistent with the states, inputs and model output data, with the center of the resultant sets representing the reference point of the estimate (Le, Stoica Manui, Alamo, Camacho, & Dumur, 2013). It is therefore necessary to represent them with compacts sets that provide less complexity from a computational point of view. Convex sets such as the interval-based set (Xiong, Jauberthie, Travé-Massuyès, & Le Gall, 2013), ellipsoidal (Liu, Zhao, & Wu, 2016), polytopic or zonotopic sets (Wang, Alamo, Puig, & Cembrano, 2018) have been used which enables estimation of sets of admissible values of states at every time instant enabling robustness to the worst-case scenario with designated a priori bounds on uncertainties (Jaulin, 2009). Some works (Combastel, 2018) goes a step further in merging the two paradigms of stochastic and set-membership methodologies to formulate a somewhat "hybrid" state estimation. Each geometrical rep-

resentation offers different characteristics which may result in ease or setbacks in computation of propagated uncertainty sets in set-based Kalman filter formulations. Zonotopes, a special class of polytopes, offer simplicity in computation of sets and flexibility in operation.

Consider the Minkowski sum of two sets S_1 and S_2 as $S_1 \oplus S_2 = \{s_1 + s_2 | s_1 \in S_1, s_2 \in S_2\}$, with a unitary box of r unitary elements, $B^r \in \mathbb{R}^r$ given as $B^r = [-1, 1]^r$. Then, a zonotope can be defined as a class of geometric set with a center p and a generator matrix $H \in \mathbb{R}^{n \times r}$ in a linear affine image as

$$\mathbb{Z} \coloneqq \langle p, H \rangle = p \oplus HB^r, \tag{2}$$

The Minkowski sum of two zonotopes $\mathbb{Z}_1 = \langle p_1, H_1 \rangle$ and $\mathbb{Z}_2 = \langle p_2, H_2 \rangle$ is thus given as:

$$\mathbb{Z}_1 \oplus \mathbb{Z}_2 \coloneqq \langle p_1, H_1 \rangle \oplus \langle p_2, H_2 \rangle = \langle p_1 + p_2, [H_1 H_2] \rangle, \tag{3}$$

The linear mapping of a zonotopic set, $\mathbb{Z}$ by a vector or a matrix $\mathcal{K}$ is given as :

$$\mathcal{K} \odot \langle p, H \rangle = \langle \mathcal{K}p, \mathcal{K}H \rangle, \tag{4}$$

and the smallest box (interval hull) containing the zonotope is described by $\square\mathbb{Z} = p \oplus rs(H)B^r$, where $rs(H)$ is a diagonal matrix such that $rs(H)_{i,j} = \sum_{j=1}^{m} |H_{i,j}|$. Hence, $\mathbb{Z} \subset \square\mathbb{Z}$.

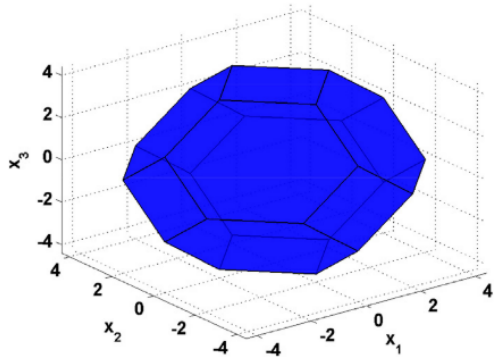

Figure 2. Zonotope in $\mathbb{R}^3$.

A linear discrete-time uncertain system with additive disturbance and noise, w_k and v_k, respectively, is considered such that:

$$x(k+1) = Ax(k) + Bu(k) + E_w w(k), \tag{5a}$$
$$y(k) = Cx(k) + E_v v(l). \tag{5b}$$

where $x \in \mathbb{R}^{n_x}$, $u \in \mathbb{R}^{n_u}$ and $y \in \mathbb{R}^{n_y}$ are states, input and output vectors, respectively. $A \in \mathbb{R}^{n_u \times n_u}$, $B \in \mathbb{R}^{n_x \times n_u}$, and $C \in \mathbb{R}^{n_y \times n_x}$ are time invariant matrices of appropriate dimensions. The process disturbance $w_k \in \mathbb{R}^{n_x}$ and the measurement noise $v_k \in \mathbb{R}^{n_y}$ are unknown but bounded in a compact set $\mathbb{W}$ and $\mathbb{V}$, respectively, with a priori specified bounds ($\bar{w}$ and $\bar{v}$) that can be formulated in a polytopic form as:

$$\mathbb{W} \coloneqq \{w(k) \in \mathbb{R}^{n_x} : |w(k) - c_w| \leq \bar{w}, c_w \in \mathbb{R}^{n_x}, \bar{w} \in \mathbb{R}^{n_x}\}, \tag{6a}$$

$$\mathbb{V} \coloneqq \{v(k) \in \mathbb{R}^{n_y} : |v(k) - c_v| \leq \bar{v}, c_v \in \mathbb{R}^{n_y}, \bar{v} \in \mathbb{R}^{n_y}\}. \tag{6b}$$

c_w, c_v, $\bar{w}$ and $\bar{v}$ are independent component-wise constants values. Zonotopic representations of the sets (6) assumed to be centered at the origin is therefore given as:

$$\mathbb{W} \coloneqq \langle 0, R_w \rangle, \tag{7a}$$
$$\mathbb{V} \coloneqq \langle 0, R_v \rangle. \tag{7b}$$

The disturbance w and noise v are assumed bounded in a unitary hypercube , $\forall w \in \mathbb{W} \coloneqq \langle 0, I_{n_w} \rangle$ and $v \in \mathbb{V} \coloneqq \langle 0, I_{n_v} \rangle$, respectively. Henceforth for purposes of notation, c and R are the center and generator matrix of zonotopes, respectively.

Assumption 3.1. The pair $[A, C]$ of the model (5) is observable.

3.2. The ZKF algorithm

The recursive procedure of the classic Kalman filter (Kalman, 1960) involves prediction of an a priori state estimation $x^-(k) = Ax^-(k-1) + Bu^-(k-1)$ and a posterior estimate, corrected by a gain K_{kf}, $x^+(k) = x^-(k) + K_{kf}(y(k) - Cx^-(k))$ under stochastic assumptions of uncertainties. In the zonotopic paradigm, the initial state is such that, $x_0 \in \mathbb{X}_0 = \langle c_0, R_{x_0} \rangle$. From the dynamic model (5), the matrices E_w and E_v are adapted as diagonal matrices with the prespecified bounds ($\bar{w}$ and $\bar{v}$) as their entries. Assuming a transition from $x(k) \in \mathbb{X}_k$ to $x(k+1) \in \mathbb{X}_{k+1}$, the a priori and posterior estimates considering zonotopic bounded uncertainty with Kalman gain K_{zk} are given as follows

A priori estimate

$$c_x^-(k+1) = Ac_x^-(k) + Bu(k), \tag{8a}$$
$$R_x^-(k+1) = [AR_x(k), E_w R_w]. \tag{8b}$$

Posterior estimate

$$c_x(k+1) = c_x^-(k+1) + K_{zk}(y(k) - Cc_x(k)), \tag{9a}$$
$$R_x(k+1) = [(I - K_z(k)C)R_x^-(k+1), -K_z(k)E_v]. \tag{9b}$$

The approach is summarized in Algorithm 1.

Algorithm 1 Zonotopic Kalman filter algorithm

Initialization: $x(0) \Longleftarrow x_0, R_x \Longleftarrow R_0, R_w$
for $k = 0 : N$ **do**
  $c_x^-(k+1) = Ac^-x(k) + Bu(k)$ ▷ Predict center
  $R_x^-(k+1) = [AR_x(k), E_wR_w]$ ▷ Predict generator matrix
  Compute the Kalman gain, $K_z(k)$
  Measure the output $y(k)$
  $c_x(k+1) = c_x^-(k+1) + K_z(k)(y(k) - Cc_x(k))$ ▷ Compute the center of the zonotope.
  $R_x^-(k+1) = [(I - K_z(k)C)R_x(k+1), -K_z(k)E_v]$ ▷ Compute the generator matrix
  $X_k = \langle c_x(k).rs(R_x(k))\rangle$ ▷ Compute the state bounding zonotope.
  $\overline{x}(k+1) = c_x(k+1) + rs(R_x(k+1))$ ▷ Maximum estimated state.
  $\underline{x}(k+1) = c_x(k+1) - rs(R_x(k+1))$ ▷ Minimum estimated state.
  end for

4. Damage Estimation of wind turbine blades Using Stiffness Degradation

4.1. Fatigue estimation background

Wind turbine blades and nacelles are commonly made of composite fibre-glass materials that ensure target static strength levels and longer service of life. As with any material, continuous exposure to stress results in a gradual loss of strength over the material lifespan eventually leading to levels below an acceptable operational condition. A number of methodologies have been used in an attempt to model a suitable damage model which predicts the eventual end of operation of wind turbine blades such as in (Leon, Kim, & Helga, 2017). Predominant amongst these methods have been the rain flow counting (RFC) and the stress degradation methods. Stiffness degradation algorithm on wind turbine blades has been comprehensively studied in (Vassilopoulos et al., 2010). This algorithm is a fatigue crack growth modelling which involves modelling and predicting the fatigue life of a composite material by considering a damage metric, usually the residual stress or residual stiffness of the material (Zhang, Vassilopoulos, & Keller, 2008), such that failure is considered when one of these metrics declines to a specified limit. This methodology considers both compressive and tensile stress functions.

4.2. Stiffness degradation method

According to (Vassilopoulos et al., 2010), the modulus decay of most fibre reinforced composite materials occurs in three stages as shown in Figure 3: E_0 is undamaged stiffness, E is the stiffness at a specific point in the material fatigue life cycle, N is the total test cycles and N_f is the fatigue life in cycles. In the first stage, there is a rapid degrading of stiffness of about 2-5% mostly due to transverse matrix cracks. Stage two involves a gradual degradation over fatigue lifetime. Damage here is mostly caused by edge delaminations and additional longitudinal cracks. Eventually in the final state, degradation occurs in abrupt steps, culminating in an overall fatigue failure of the specimen.

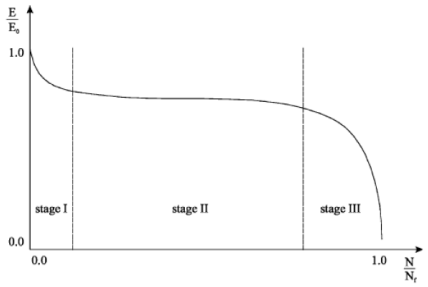

Figure 3. Curve showing stages of stiffness degradation.

From (Van Paepegem & Degrieck, 2002), under the assumption that the blade is a solid beam, the damage model considering compressive stress can be described as:

$$\frac{dD}{dN} = f_i(\phi, D) + f_p(\phi, D), \tag{10}$$

where f_i is the initial stage function of steep decline in stiffness, f_p is the damage propagation function of the second and final stages and ϕ. These two functions are given by

$$f_i(\phi, D) = \left[C_1\Sigma(\phi, D)\exp(-C_2\frac{D}{\sqrt{\Sigma(\phi, D)}})\right]^3, \tag{11a}$$

$$f_p(\phi, D) = C_3D\Sigma(\phi, D)^2\left[1 + \exp(\frac{C_5}{3}(\Sigma(\phi, D) - C_4)\right]. \tag{11b}$$

where failure index $\Sigma(\phi, D)$ is a function of the damage D resulting in material strength reduction and the stress value ϕ

$$\Sigma(\phi, D) = \frac{\phi}{(1-D)X_c}. \tag{12}$$

The constant X_c is the comprehensive static strength. The damage growth model from initiation to final fatigue failure is thus given as :

$$\frac{dD}{dN} = \left[C_1\Sigma\exp(-C_2\frac{D}{\sqrt{\Sigma}})\right]^3 + C_3D\Sigma^2\left[1+\exp(\frac{C_5}{3}(\Sigma - C_4)\right] \tag{13}$$

where C_1 and C_2 are the material constants, C_3 is the damage propagation rate, C_4 is a threshold below which there is no initiation of fibre fracture. When the threshold C_4 is crossed, the initial fibre fracture occurs on the specimen, which causes an exponential rapid decrease in strength and enables the final fatigue failure of the material. As long as the failure index is below the threshold C_4, the parameter C_5 assumes a large value to ensure a strongly negative exponential func-

tion. When C_4 is crossed, it assumes a large positive for accelerated degradation of the material. The third power is used for compressive stress as they show from experiments to have considerably less effect than tensile stress (Sanchez-Sardi et al., 2016). From (Van Paepegem & Degrieck, 2002), the parameters for a damage model for a fibre-reinforced composite of which wind turbine blades are made up of with the stiffness degradation algorithm is given in the Table 1

Table 1. Parameters for stiffness degradation model.

Parameter	Value	Unit
C_1	0.002	(1/cycle)
C_2	30	-
C_3	4×10^{-4}	(1/cycle)
C_4	0.85	-
C_5	93	-
X_c	341.5	Mpa

4.3. Prediction of end of life

The events in time, the EOL and RUL are calculated as bounded sets of possible values, which are calculated at a specified time k_p, with predicted states from the ZKF considering uncertainties. Therefore, the prediction of $\square EOL(x(k_p)|y(k_p))$ and $\square RUL(x(k_p)|y(k_p))$ is dependent on the estimation of bounded states for damage propagation using the stiffness degradation method in (13). From the ZKF, the estimated center of the zonotope is used for the prognosis procedure, where it is propagated in future time till it reaches a predefined threshold. Keeping in mind that future evolution of states in this prognosis is subject to uncertainty, the uncertainties are assumed unknown but bounded in a zonotope, such that the resultant EOL and hence the RUL is bounded in a set. Given $\{x(k_p) := c_{x_{k_p}})\}_{i=0}^{N}$, which is the estimated center from the Kalman filter, an estimate of the propagated damage from the stiffness degradation method is evaluated until the strength of the UUT degrades to a predefined limit. Hence, when $T_{EOL}(D(x(k)) = 1$, which is dependent on the strength degradation function $D(x(k))$. With states and bounds evaluated from Algorithm 1, the prediction of the EOL is summarised in Algorithm 2.

Algorithm 2 Prediction of EOL

Inputs $\{(x(k_p), R_x(k_p), R_w\}$
Output $\{EOL, \overline{EOL}, \underline{EOL}\}$
$c(k) \longleftarrow x(k_p)$
$[k_{cen}, k_{min}, k_{max}] \longleftarrow k_p$
for $i = k : N$ **do**
  while $T_{EOL}(\underline{D_{k_{min}}(k)}) = 0$ **do**
    $D_{cen}(k) \longleftarrow D(c(k))$ ▷ Propagation of damage center
    $\underline{D_{min}}(k) \longleftarrow D(c(k) - rs(R_x(k)))$ ▷ Propagation of damage lower bound
    $\overline{D_{max}}(k) \longleftarrow D(c(k) + rs(R_x(k)))$ ▷ Propagation of damage upper bound
    $c(k+1) = Ac(k) + Bu(k)$ ▷ Propagation of states
    $R_x(k+1) = [AR_x(k) \quad R_w E_w]$ ▷ Propagation of uncertainty bounds
    if $T_{EOL}(\underline{D_{k_{cen}}}) = 0$
      then $\underline{k_{cen}} \longleftarrow k_{cen} + 1$
    if $T_{EOL}(\underline{D_{k_{min}}}) = 0$
      then $\underline{k_{min}} \longleftarrow k_{min} + 1$
    if $T_{EOL}(\underline{D_{k_{max}}}) = 0$
      then $\underline{k_{max}} \longleftarrow k_{max} + 1$
  End while
  $\underline{EOL} \longleftarrow k$
  $\overline{EOL} \longleftarrow k_{min}$
  $\underline{EOL} \longleftarrow k_{max}$
End for

5. Case Study

In this section, the monitored system under study, a wind turbine of rated power 5MW is described. Subsequently, a control oriented model which captures key dynamics of the system is then presented.

5.1. Wind turbine model

A wind turbine functions by utilizing energy from wind to produce electric power. The aerodynamics of the wind turbine is governed by the wind turbine's blade by means of the blade pitch angle β, producing speed in the rotor with an associated aerodynamic torque. This aerodynamic torque is then transferred from the rotor to the generator through the drive train to produce electric power at different operating conditions by manipulating the blade pitch angle and the generator torque. The wind turbine operates in three regions, dependent on the magnitude of the wind speed to produce electric power from captured wind. Considering rated wind speed V_{rated} as $12m/s$, when wind speeds, $v_s(t) \leq 12m/s$, the pitch angle is maintained at 0°, allowing for maximum exposure of the blades to wind for utmost energy available. Therefore below V_{rated}, only the reference torque actuator is operational. For $v_s(t) \geq 12m/s$ but less than the cut-off wind speed, $25m/s$, the blade actuator varies accordingly to information of the varying wind, such that the blade angle of attack is reduced accounting for less and regulated energy from wind to ensure rated power without overspeeding, protecting plant components. In this region, both the torque (T_g) and the rotor speed (w_r) is kept at their respective rated values. At wind speeds greater than the cut-off, the wind turbine ceases to operate. Neglecting torsion angle and friction and with the assumption that the low and high speed shaft are one complete model, the non-linear model of the wind turbine is described as:

$$\dot{w_r} = \frac{1}{J}(T_a - N_g T_g), \tag{14a}$$

$$\ddot{V_t} = \frac{1}{M_t}(T_r - K_t V_t - B_t \dot{V_t}), \tag{14b}$$

$$\dot{\beta} = \frac{1}{\tau_p}(-\beta + \beta_r), \tag{14c}$$

$$\dot{T_g} = \frac{1}{\tau_g}(-T_g + T_{g_r}), \tag{14d}$$

where w_r is the rotor speed, T_g is the generator torque, β, the pitch angle for capturing wind depending on wind speeds, V_t and $\dot{V_t}$ is the the nacelle fore-aft velocity from the tower oscillations. The model parameters J, N_g, M_t, K_t, B_t, τ_p and τ_g are the rotor inertia, gear ratio, the tower fore-aft inertia, the tower fore-aft rigidity, the mechanical damping, the time constant of the pitch and the time constant of the generator, respectively. The rotor and aerodynamic torques (T_r and T_a) which are dependent on the power and thrust coefficients C_p and C_q, both of which are functions of the pitch angle β and blade tip speed λ are given as:

$$T_a = \frac{1}{2}\rho\pi R^3 \frac{C_p(\lambda,\beta)}{\lambda} v_s^2, \tag{15a}$$

$$T_r = \frac{1}{2}\rho\pi R^2 C_q(\lambda,\beta) v_s^2, \tag{15b}$$

$$\lambda = \frac{R w_r}{v_s}. \tag{15c}$$

5.2. Linearized model

For purpose of the Kalman filter, a suitable linearized model is presented at the following working points, $v_s^* = 14m/s$, $w_r^* = 1.2571hz$, $T_g^* = 43093.5Nm$ and $\beta^* = 4^\circ$. With parameters from (P.F. Odgaard & Kinnaert., 2009), the nonlinear model (14)-(15) can be estimated by a discrete linear model with a sampling time of T_s as:

$$x(k+1) = Ax(k) + Bu(k) + Ew(k), \tag{16a}$$

$$y(k) = Cx(k). \tag{16b}$$

such that the linearized time invariant system matrices using the Euler discretization are given as follows:

$$A = \begin{bmatrix} -0.0556 & 0 & -0.0263 & -0.008 & -2.3\times10^6 \\ 0 & 1 & 0 & 0 & 0 \\ 0.815 & -4.240 & -0.2094 & -0.1427 & 0 \\ 0 & 0 & 0 & -50 & 0 \\ 0 & 0 & 0 & 0 & -50 \end{bmatrix}$$

$$B = \begin{bmatrix} 0 & 0 \\ 0 & 0 \\ 0 & 0 \\ 0 & 50 \\ 50 & 0 \end{bmatrix},$$

$$E = \begin{bmatrix} 0.0263 & 0 & 0.1871 & 0 & 0 \end{bmatrix}^T,$$

$$C = \begin{bmatrix} 1 & 0 & 0 & 0 & 0 \\ 0 & 0 & 0 & 1 & 0 \\ 0 & 0 & 0 & 0 & 1 \end{bmatrix}.$$

6. RESULTS

Simulations are performed considering wind speeds, $12m/s \geq v_s(t)m/s \leq 25m/s$; at the region of rated power. The reference pitch angle β_r, is kept constant and hence the control inputs $u(t) = [T_{g_r}, \beta_r]$ are kept constant throughout the simulation with a corresponding wind speed of $14m/s \geq v_{rated}$, such that only the states vary under the presence of unknown uncertainties. To evaluate the efficacy of the proposed scheme, it is compared with estimation from the generic Kalman filter, where states in both cases are estimated for purposes of damage propagation using the stiffness degradation model (13). For comparison purposes, the predefined bounds are chosen based on the statistical properties of the Kalman filter, such that symmetric interval bounds are considered, $w_i(t) \in \mathbb{R} \subseteq [-3\sigma_{w_i}, 3\sigma_{w_i}]$ and $v_i(t) \in \mathbb{R} \subseteq [-3\sigma_{v_i}, 3\sigma_{v_i}], \forall i = [1,3]. i \in \mathbb{N}$, where σ_{w_i} and σ_{v_i} are standard deviations from the Kalman filter. These bounds are used for description of the zonotopic sets and random selection of uncertainty values for simulations.

The blade root moment is chosen as the the stress function ϕ for the damage model (13), which is modelled by (Sanchez-Sardi et al., 2016), as a first order time varying linear function of the generated power, $P = n_g T_g w_r$, and wind speed v_s. The stress input is therefore taken as:

$$M_b(k) = a_1 P(k) + a_2 v_s(k) + a_3 \tag{17}$$

with parameters, $a_1 = 757.52$, $a_2 = -248.83$ and $a_3 = 6468$. The EOL of the blade composite material is chosen as 0.8, which signifies the number of cycles of stress inputs until an 80% reduction in the blade material's strength as shown in Figure 4.

Performance of the estimation is compared at different conditions of varied noise magnified by factors (N) of 1,10,100 and 500. The comparison criterion for estimation is evaluated using the percent root mean square error. From Tables 3 and 4 on the robustness of the Kalman filters to scaled noise values, it is could be realised that performance as expected deteriorates when the magnitude of noise is increased but the ZKF shows better performance under these conditions due its lesser conservativeness as compared to the generic Kalman filter. The relative accuracy (RA) as proposed in (A Saxena & Saha ., 2009) is used as a performance metric for the RUL.

From the Tables 3 and 4, on the values of the RA, the ZKF proves to be more accurate and precise in calculating the RUL under scaled noise values. Simulation is run for 3000 secs

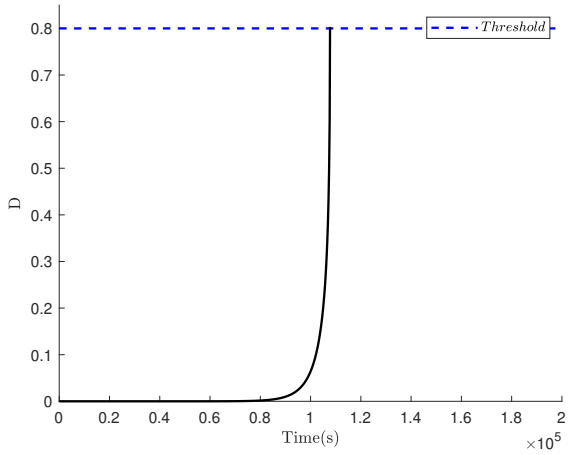

Figure 4. Stiffness degradation to a predefined threshold.

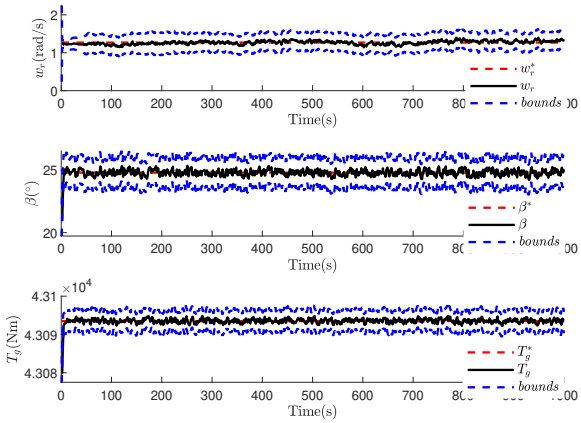

Figure 5. ZKF estimation of states with bounds.

with sampled estimated states used every 60s for the prediction of the EOL and thus the RUL. Such that predicted states which are inputs to the degradation function is propagated with uncertainties in the prognosis procedure as shown in Figure 7, where the bounded estimated power propagation failure is shown. The average of these EOL estimates is used together with its bounds for evaluating a bounded RUL in Figure 8.

Table 2. Performance of ZKF

N	$PRMSE_{w_r}$	$PRMSE_{\beta}$	$PRMSE_{T_g}$	RA
1	1.15	0.32	0.97	98.7
10	1.18	0.31	0.96	98.5
100	1.35	1.74	2.29	98.2
500	2.05	3.59	4.23	97.3

Table 3. Performance of KF

N	$PRMSE_{w_r}$	$PRMSE_{\beta}$	$PRMSE_{T_g}$	RA
1	0.41	0.21	0.75	98.9
10	1.3	0.42	1.31	98.2
100	3.92	18.53	36.7	95.1
500	13.65	55.89	137	62.4

7. CONCLUSIONS

It is important to take into account the effects of uncertainties when predicting the EOL and thus the RUL of a UUT, due to the critical nature of these information for operational decisions. Therefore, in this paper a zonotopic Kalman filter for the purpose of estimating states for prognosis of a wind turbine blade is designed. Uncertainties from process disturbance and noise are assumed unknown but bounded in zonotopic sets from predefined symmetric bounds. These sets

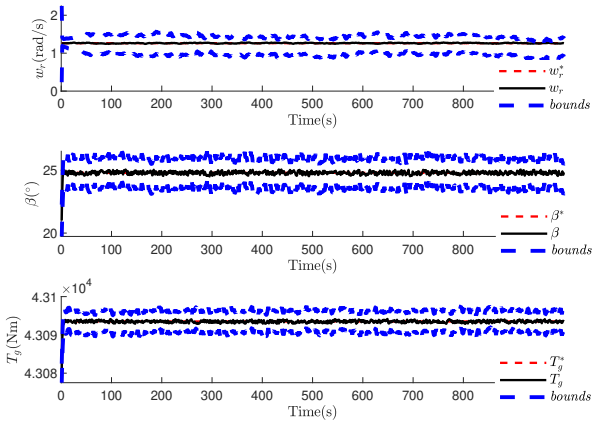

Figure 6. KF estimation of states with bounds.

enables a bounded estimation of states by means of the recursive Kalman filter process using a set-based method, with the center and bounds of these sets subsequently used as inputs to the nonlinear function of a stiffness degradation model to evaluate a bounded EOL and RUL of of wind turbine blades. The process of estimating the states and therefore the EOL and RUL is compared with a prognosis procedure using the generic Kalman filter under the same conditions of disturbance and noise from the statistical properties of the standard Kalman filter. Observations from this study showed a similar performance in prediction of damage under nominal conditions, but the zonotopic Kalman filter showed more accuracy when noise levels were increased and therefore an accuracy in estimation of states. The resultant bounded RUL will therefore aid in enabling optimal operational decisions on the health of wind turbine blades, for example to consider the lower bound of the RUL when conservative decision on the blade's health are to be taken.

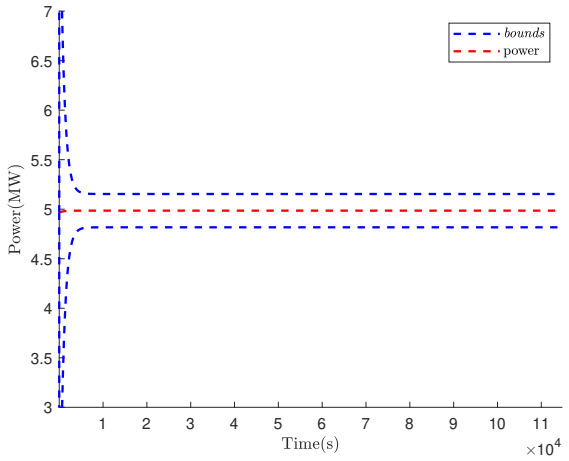

Figure 7. Propagated power in one sample of prognosis.

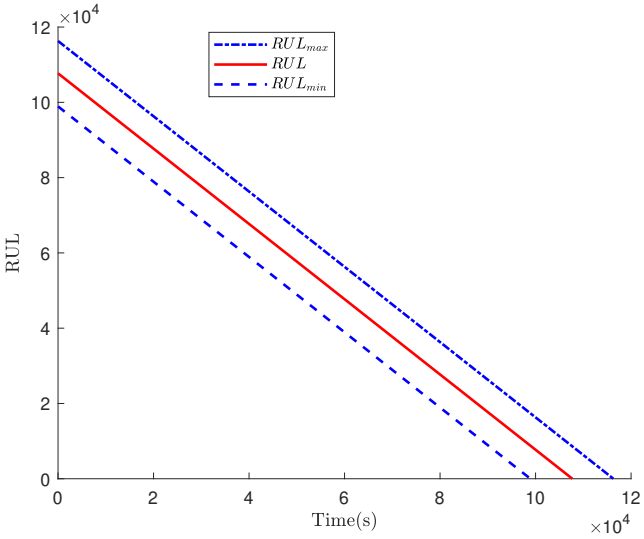

Figure 8. Bounded RUL using ZKF.

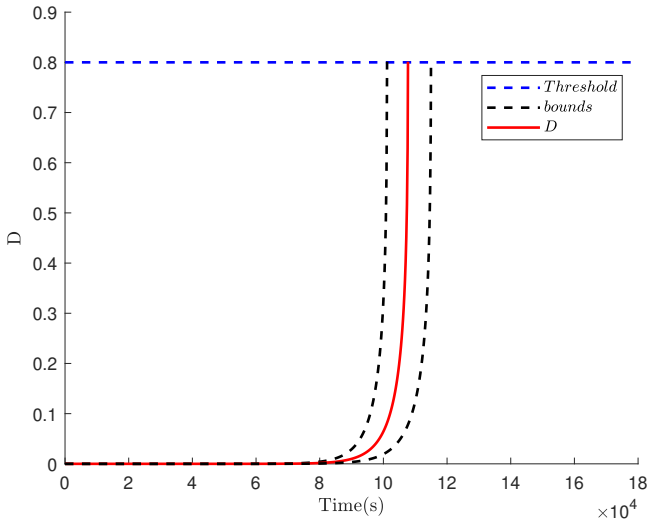

Figure 9. Bounded stiffness degradation to predefined threshold using ZKF.

ACKNOWLEDGMENT

This work has been funded by the Spanish State Research Agency (AEI) and the European Regional Development Fund (ERFD) through the project SCAV (ref. MINECO DPI2017-88403-R), by the DGR of Generalitat de Catalunya (SAC group ref. 2017/SGR/482) and by SMART Project (ref. num. EFA153/16 Interreg Cooperation Program POCTEFA 2014-2020).

REFERENCES

A Saxena, J. C., & Saha ., B. (2009). On applying the prognostic performance metrics. In *Paper presented at the annual conference of the prognostics and health management society, san diego, california, usa, 27 september–1 october 2009.*

Combastel, A., C. Zolghadri. (2018). Fdi in cyber physical systems: A distributed zonotopic and gaussian kalman filter with bit-level reduction. *IFAC Paper online*, 776-783. doi: 10.1109/CDC.2013.6759929

Daigle, M., Saha, B., & Goebel, K. (2012). A comparison of filter-based approaches for model-based prognostics. *2012 IEEE Aerospace Conference*, 1-10.

Ferreira, J., Balthazar, J., & Araujo, A. (2003). An investigation of rail bearing reliability under real conditions of use. *Engineering Failure Analysis.*, *10*, 745–758.

Gu, J., Barker, D., & Pecht, M. G. (2007). Uncertainty assessment of prognostics of electronics subject to random vibration. In *Aaai fall symposium: Artificial intelligence for prognostics.*

IRENA. (2012). *Renewable energy technologies: cost analysis series* (Vol. 1; Tech. Rep. No. 5/5). International Renewable Energy Agency.

Jaulin, L. (2009, 06). Robust set membership state estimation ; application to underwater robotics. *Automatica*, *45*, 202-206. doi: 10.1016/j.automatica.2008.06.013

Kalman, R. E. (1960). A new approach to linear filtering and prediction problems. *ASME Journal of Basic Engineering*.

Le, V., Stoica Manui, C., Alamo, T., Camacho, E., & Dumur, D. (2013, 11). Zonotopic guaranteed state estimation for uncertain systems. *Automatica*, *49*. doi: 10.1016/j.automatica.2013.08.014

Leon, M., Kim, B., & Helga, N. (2017). Materials for wind turbine blades: An overview. *Materials (Basel).*, *15*(10(11)), 244-259.

Liu, Y., Zhao, Y., & Wu, F. (2016). Ellipsoidal state-bounding-based set-membership estimation for linear

system with unknown-but-bounded disturbances. *IET Control Theory Applications*, *10*(4), 431-442.

Madhav, M. (2015). *Model-based prognostics for prediction of remaining useful life* (Unpublished doctoral dissertation). Luleåa University of Technology.

P.F. Odgaard, J. S., & Kinnaert., M. (2009). Fault tolerant control of wind turbines - a benchmark model. In *Proceedings of 7th ifac symposium on fault detection, supervision and safety of technical processes. barcelona, spain, 2009.*

Sanchez-Sardi, H., Sankararaman, S., Escobet, T., Puig, V., Frost, S., & Goebel, K. (2016, 07). Analysis of two modeling approaches for fatigue estimation and remaining useful life predictions of wind turbine blades. In *3rd european phm 2016.*

Tsui, K., Chen, N., Zhou, Q., Hai, Y., & Wang, W. (2015, 05). Prognostics and health management: A review on data driven approaches. *Mathematical Problems in Engineering*, *2015*, 1-17. doi: 10.1155/2015/793161

Van Paepegem, W., & Degrieck, J. (2002). A new coupled approach of residual stiffness and strength for fatigue of fibre-reinforced composites. *INTERNATIONAL JOURNAL OF FATIGUE*, *24*(7), 747–762.

Vassilopoulos, A., Brøndsted, P., & Nijssen, R. (Eds.). (2010). *Advances in wind turbine blade design and materials*. Woodhead Publishing Limited, Cambridge.

Wang, Y., Alamo, T., Puig, V., & Cembrano, G. (2018). A distributed set-membership approach based on zonotopes for interconnected systems. *2018 IEEE Conference on Decision and Control (CDC)*, 668-673.

Xiong, J., Jauberthie, C., Travé-Massuyès, L., & Le Gall, F. (2013, 12). Fault detection using interval kalman filtering enhanced by constraint propagation. *Proceedings of the IEEE Conference on Decision and Control*, 490-405. doi: 10.1109/CDC.2013.6759929

Zhang, H., Kang, R., & Pecht, M. (2009). A hybrid prognostics and health management approach for condition-based maintenance. *2009 IEEE International Conference on Industrial Engineering and Engineering Management*, 1165-1169.

Zhang, Y., Vassilopoulos, A., & Keller, T. (2008, 10). Stiffness degradation and fatigue life prediction of adhesively-bonded joints for fiber-reinforced polymer composites. *International Journal of Fatigue*, *30*, 1813–1820. doi: 10.1016/j.ijfatigue.2008.02.007